On Lithium-6 as a Diagnostic of the Lithium-enrichment Mechanism in Red Giants

Claudia Aguilera-Gómez[1] , Julio Chanamé[2,3] , and Marc H. Pinsonneault[4]

[1] Departamento de Ciencias Físicas Universidad Andrés Bello, Fernandez Concha 700, 759-1538, Las Condes, Santiago, Chile; craguile@uc.cl
[2] Instituto de Astrofísica, Pontificia Universidad Católica de Chile, Av. Vicuña Mackenna 4860, 782-0436 Macul, Santiago, Chile
[3] Millennium Institute of Astrophysics, Santiago, Chile
[4] Department of Astronomy The Ohio State University, Columbus, OH 43210, USA

Abstract

High lithium-7 (^{7}Li) abundances in giants are indicative of nonstandard physical processes affecting the star. Mechanisms that could produce this signature include contamination from an external source, such as planets, or internal production and subsequent mixing to the stellar surface. However, distinguishing between different families of solutions has proven challenging, and there is no current consensus model that explains all the data. The lithium-6 (^{6}Li) abundance may be a potentially important discriminant, as the relative ^{6}Li and ^{7}Li abundances are expected to be different if the enrichment were to come from internal production or from engulfment. In this work, we model the ^{6}Li and ^{7}Li abundances of different giants after the engulfment of a substellar mass companion. Given that ^{6}Li is more strongly affected by Galactic chemical evolution than ^{7}Li, ^{6}Li is not a good discriminant at low metallicities, where it is expected to be low in both star and planet. For modeled metallicities ([Fe/H] > −0.5), we use a "best-case" initial ^{6}Li/^{7}Li ratio equal to the solar value. ^{6}Li increases significantly after the engulfment of a companion. However, at metallicities close to solar and higher, the ^{6}Li signal does not last long in the stellar surface. As such, detection of surface ^{6}Li in metal-rich red giants would most likely indicate the action of a mechanism for ^{6}Li enrichment other than planet engulfment. At the same time, ^{6}Li should not be used to reject the hypothesis of engulfment in a ^{7}Li-enriched giant or to support a particular ^{7}Li-enhancement mechanism.

Unified Astronomy Thesaurus concepts: Red giant stars (1372); Solar-planetary interactions (1472); Lithium stars (927); Low mass stars (2050); Stellar evolutionary models (2046)

1. Introduction

Lithium-7, one of the two stable isotopes of lithium (Li), was produced right after the Big Bang, and it is used to understand element production in the early universe (Coc et al. 2014), diagnose mixing in stellar interiors (Pinsonneault 1997), and study galactic chemical evolution (Prantzos et al. 2017), among other applications.

In low-mass stars, Li is destroyed in the interior during the main sequence. When stars evolve to the red giant branch (RGB), during the first dredge-up the outer convection zone deepens in mass, diluting the ^{7}Li left close to the stellar surface. For this reason, high ^{7}Li abundances in giants require the presence of nonstandard mechanisms modifying the abundance of the star.

One possible explanation for high surface ^{7}Li in red giants relies on the efficient transport by extra mixing of ^{7}Li produced through the Cameron–Fowler mechanism (Cameron & Fowler 1971). Another explanation for the enhanced ^{7}Li is the contamination from a source that preserves or creates ^{7}Li, such as supernovae (Martin et al. 1994) or substellar companions (e.g., Siess & Livio 1999). An evolved companion, such as an asymptotic giant branch star, which produces ^{7}Li during its thermal pulses (Sackmann & Boothroyd 1992) could also be a source of Li. However, the small fraction of Li-rich giants that have been searched for binary companions do not seem to show evidence of them (Aguilera-Gómez 2018, Chapter 3.1). Further work is needed to test this possibility for the majority of red giants.

In Aguilera-Gómez et al. (2016a), we modeled the engulfment of different planets and brown dwarfs by giant stars. We found that engulfment of substellar companions (SSCs) can explain ^{7}Li abundances as high as $A(^7\text{Li}) = 2.2$,[5] and that the threshold for defining what is enriched and what is normal depends on stellar mass and metallicity. In addition, as giants with higher surface ^{7}Li are found in nature (e.g., Yan et al. 2018; Deepak & Reddy 2019), Aguilera-Gómez et al. (2016a) concluded that different ^{7}Li-enrichment mechanisms are needed to explain the entire population. Recent survey data provide additional observational support for these conclusions (Martell et al. 2020).

Other observational indicators can be used to distinguish between ^{7}Li replenishment scenarios. The evolutionary phase of the enriched giants is an important indicator of the physical conditions where the enrichment is produced. Some works, such as Deepak & Reddy (2019) and Casey et al. (2019), argued that most of these unusual giants are located in the horizontal branch. This could point to a mechanism of ^{7}Li enrichment working close to the RGB tip or during the helium flash. On the other hand, measurements of the stellar rotation (Carlberg et al. 2012), beryllium surface abundance (Takeda & Tajitsu 2017), and carbon isotopic ratio (Tayar et al. 2015) could all be fundamental in finding the mechanism behind the ^{7}Li enrichment.

Another potentially important probe could be ^{6}Li, the far-less-abundant stable isotope of Li, thought to be primarily produced by cosmic-ray spallation (Meneguzzi et al. 1971).

As ^{6}Li is destroyed in stellar interiors at even lower temperatures than those required to burn ^{7}Li (Brown & Schramm 1988), standard stellar evolutionary models predict much more severe burning of ^{6}Li than ^{7}Li at any evolutionary

---

[5] $A(x) = \log(n_x/n_H) + 12$.

1

state (Proffitt & Michaud 1989), and very low surface ^{6}Li abundances during the RGB.

In contrast, planets and brown dwarfs preserve their initial ^{6}Li, so the abundance of this isotope should be higher in giants that have engulfed their companions. On the contrary, the Cameron–Fowler mechanism is not able to produce ^{6}Li. Thus, it may be possible to use ^{6}Li to identify candidates of planet engulfment (Charbonnel & Balachandran 2000).

^{6}Li can also be produced in stellar flares (Montes & Ramsey 1998) and Galactic cosmic-ray interaction with the interstellar medium (Fields & Olive 1999). It is possible that the Sun is producing ^{6}Li through flares, based on the high abundances found on the lunar soil (Chaussidon & Robert 1999). However, no ^{6}Li is found in the surface of the Sun, implying that even if some part of the ^{6}Li created is preserved in the photosphere, it is not enough to be measured. In giants, there is an additional difficulty, given the large convective envelope that would dilute the ^{6}Li created by any mechanism, complicating its detectability.

Given the complications associated with the production of ^{6}Li through flares, engulfment is one of the more cited ^{6}Li-enrichment mechanisms in the literature. Also, because of the large constrast of ^{6}Li pre- and post-engulfment, the planet signal could be easier to detect than that of ^{7}Li. However, at lower metallicities, chemical evolution effects predict very low birth planetary abundances and the fragility of ^{6}Li implies that it could be burned even where ^{7}Li is stable. To analyze if ^{6}Li can effectively be used as a diagnostic of engulfment for all giants, we model the ^{6}Li abundance after the engulfment of SSCs of different properties (Section 2). The resulting ^{6}Li surface abundance (Section 3) shows that stellar metallicity plays an important role in the burning of ^{6}Li under convective conditions, with higher-metallicity stars very rapidly burning their original ^{6}Li and that deposited by the planet. Consequently, the absence of this isotope in the surface of ^{7}Li-rich giants cannot be used to reject the SSC engulfment hypothesis. We analyze in detail this result in Section 4, to finally summarize in Section 5.

2. Models

We follow a similar procedure to that described in Aguilera-Gómez et al. (2016a). We refer the reader to that work for an in-depth analysis of the assumptions, the calculation of point of SSC dissipation in stellar interiors, and the parameters used in our grid of stellar models.

In summary, we use a post-processing approach, where standard stellar evolution models are used as a base to later implement the engulfment and thus there is no feedback from the planet ingestion process. Standard stellar models are obtained with the Yale Rotating Evolutionary code (Pinsonneault et al. 1989).

The modeled stellar mass goes from 1.0 to 2.0 $M_\odot$. Metallicities range from [Fe/H] = −0.5 to [Fe/H] = 0.18 and giants are evolved to the tip of the RGB. We do not consider lower metallicities because the normal Galactic chemical evolution trends would predict a smaller than solar birth ^{6}Li/^{7}Li ratio. In such stars, an engulfed planet is likely to supply little ^{6}Li due to its low birth ^{6}Li. Thus, the low overall ^{6}Li would make this signal impossible to observe. Low-metallicity stars are also known to experience severe in situ Li depletion on the giant branch. This combination makes ^{6}Li a

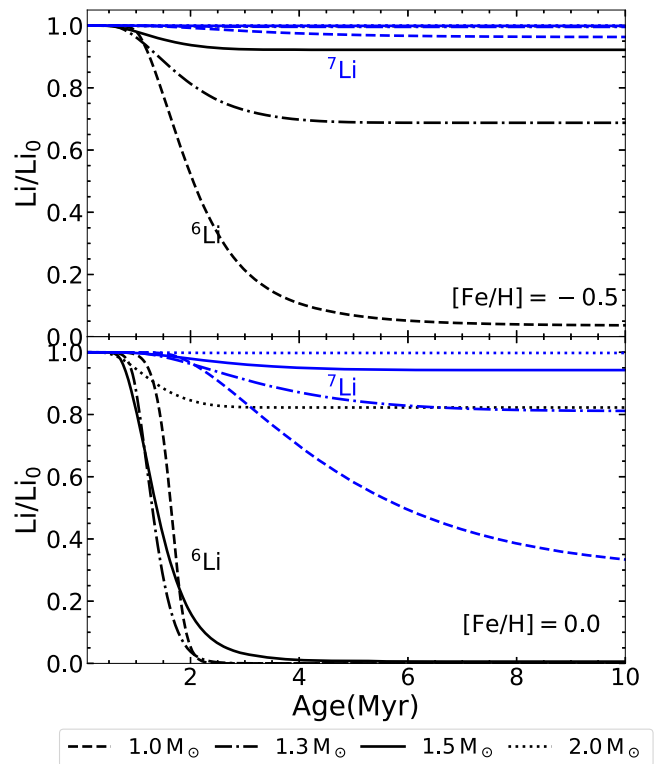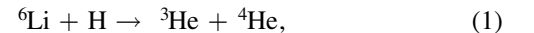**Figure 1.** ^{6}Li (black) and ^{7}Li (blue) over Li_0, the meteoritic Li abundance, in the pre-main sequence of stars of four different masses, at metallicities [Fe/H] = −0.5 (top panel) and [Fe/H] = 0.0 (bottom panel).

poor discriminant for metal-poor progenitors, and we therefore focus on higher-metallicity stars.

The ^{6}Li in stellar interiors is burned through the reaction

$$^6\text{Li} + \text{H} \rightarrow \ ^3\text{He} + \ ^4\text{He}, \tag{1}$$

with reaction rates from Lamia et al. (2013).

Regarding the stellar initial ^{6}Li abundance in our models, we consider a fixed meteorite Li isotopic ratio ^{6}Li/^{7}Li = 0.082 (Chaussidon & Robert 1998). Because ^{6}Li should increase with metallicity due to the contribution of cosmic-ray spallation (e.g., Prantzos 2012), the birth ^{6}Li is expected to be lower at lower metallicity. We therefore regard this as an optimistic case scenario, where engulfed objects will give the maximum signal. We note, however, that our differential depletion calculations are independent of the assumed birth ratio, given that the ^{6}Li and ^{7}Li depletion factors, defined as the fraction of initial Li remaining in the surface of the star, are independent of the birth values.

The initial ^{6}Li value is set before the expected phase of Li burning in the pre-main sequence; thus, the Li isotopic ratio can drastically change in this phase. Figure 1 shows the burning of Li in the pre-main sequence for stars of different mass and metallicities of [Fe/H] = −0.5 (top) and [Fe/H] = 0.0 (bottom panel). Higher-mass stars preserve their ^{6}Li/^{7}Li, while there is more burning in solar-metallicity stars. Li_0 here is the meteoritic Li abundance assumed.

To better control for the effect of Li burning previous to the RGB phase, we quantify the Li abundances at the zero-age main sequence. Although there is some burning of ^{6}Li during the main sequence, the main depletion process takes place before that. Figure 2 shows the ^{7}Li and ^{6}Li depletion factors at the zero-age main sequence, for stars of different masses and

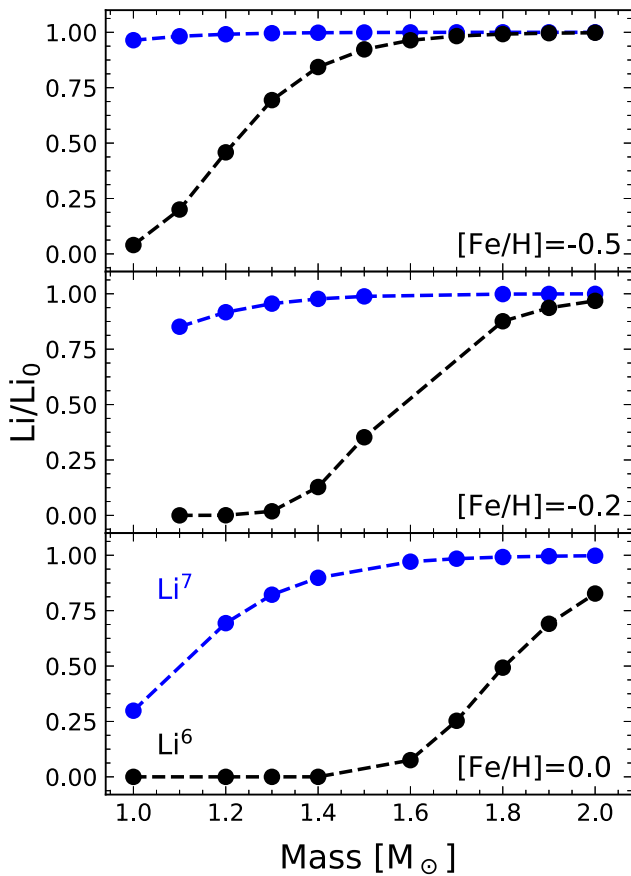**Figure 2.** ^{6}Li (black) and ^{7}Li (blue) depletion factors at the zero-age main sequence (i.e., due to pre-main-sequence evolution) for stars of different masses. The panels show results for specific metallicities.

metallicities. There is little to no depletion at higher masses, but important depletion for ^{6}Li at low masses at any metallicity. ^{7}Li also burns considerably in low-mass stars at higher metallicities.

For the SSC, we use a fixed ratio between ^{6}Li mass fraction and metals equal to the solar system meteoritic value. Thus, all SSCs have the same $X_{^6\text{Li}}/Z$ but could have a different metal content, changing its mass fraction of ^{6}Li. The metal content of SSCs depends on their mass. Details can be found in Aguilera-Gómez et al. (2016a). Results from that work show that very massive brown dwarfs dissolve in the stellar radiative interior rather than in the convective envelope. Because of that, we decide to model SSC masses up to 15 M_J. At higher metallicities the maximum mass of a companion that still dissolves in the convective zone increases (Aguilera-Gómez et al. 2016b).

3. ^{6}Li Abundance Evolution

We begin by considering the engulfment of four SSCs by 1.3 $M_\odot$ and 1.8 $M_\odot$ red giants of [Fe/H] = −0.5, and a 1.7 $M_\odot$ of [Fe/H] = 0.05. The companions correspond to a 15 M_J brown dwarf with $Z = Z_\odot$, a 15 M_J brown dwarf with $Z = 2.5Z_\odot$, a Jupiter-like planet with $Z = 2.5Z_\odot$, and an Earth-like planet ($Z = 1$).

Several different engulfment times were modeled. However, since the ^{6}Li abundance post-engulfment can change due to burning at any time and due to dilution during the first dredge-
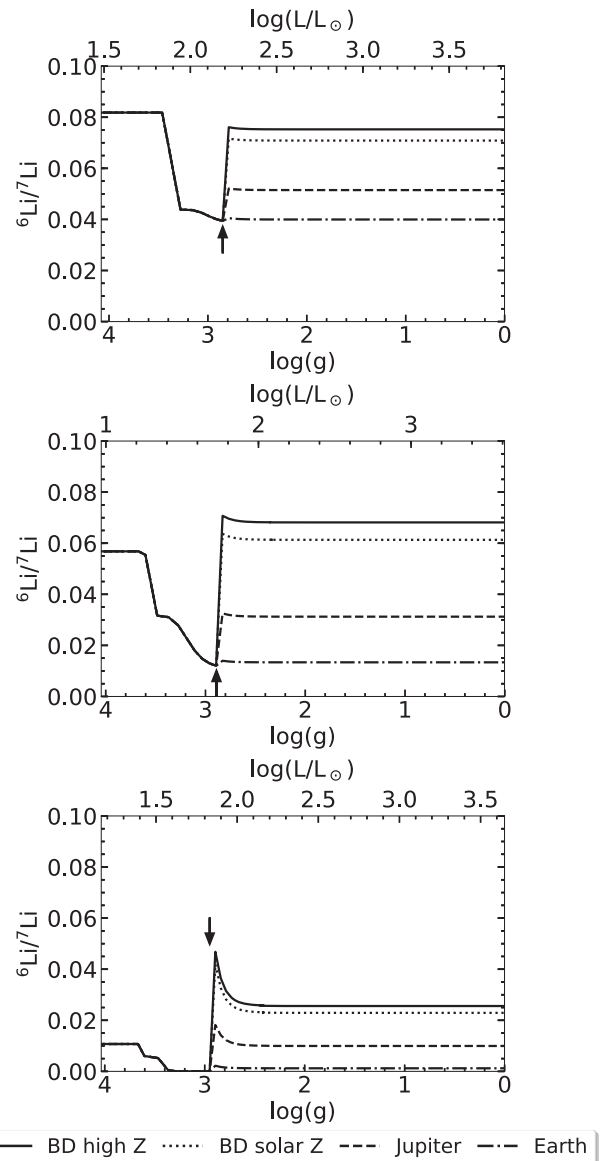

Figure 3. Surface ^{6}Li/^{7}Li evolution in a 1.8 $M_\odot$ star (top panel) and a 1.3 $M_\odot$ star (middle panel) of [Fe/H] = −0.5, and a 1.7 $M_\odot$ giant of [Fe/H] = 0.05 (bottom panel) after the engulfment of four different SSCs. The arrow shows the location of the engulfment event. The ^{6}Li/^{7}Li at the start of the RGB is different from the meteoritic ^{6}Li/^{7}Li = 0.082 due to pre-main-sequence burning.

up, we show the case of engulfment right after the end of the first dredge-up. This way, the effects of standard dilution are not present anymore, and the evolution of ^{6}Li post-engulfment is simpler to interpret.

The evolution of the ^{6}Li/^{7}Li surface ratio for these stars can be seen in Figure 3 as a function of luminosity and log g. The ^{6}Li in the main sequence can be lower than the meteoritic value due to pre-main-sequence burning. The ^{6}Li/^{7}Li ratio decreases during the first dredge-up (log $g \sim 3.5$), as expected. This is produced because right below the convective envelope, ^{6}Li burns more rapidly than ^{7}Li. When the first dredge-up mixes that material into the surface, the ^{6}Li is reduced by a larger amount than ^{7}Li.

The ratio ^{6}Li/^{7}Li increases after the engulfment of planets (at log $g \sim 2.9$ in Figure 3). The ^{6}Li enrichment is larger for
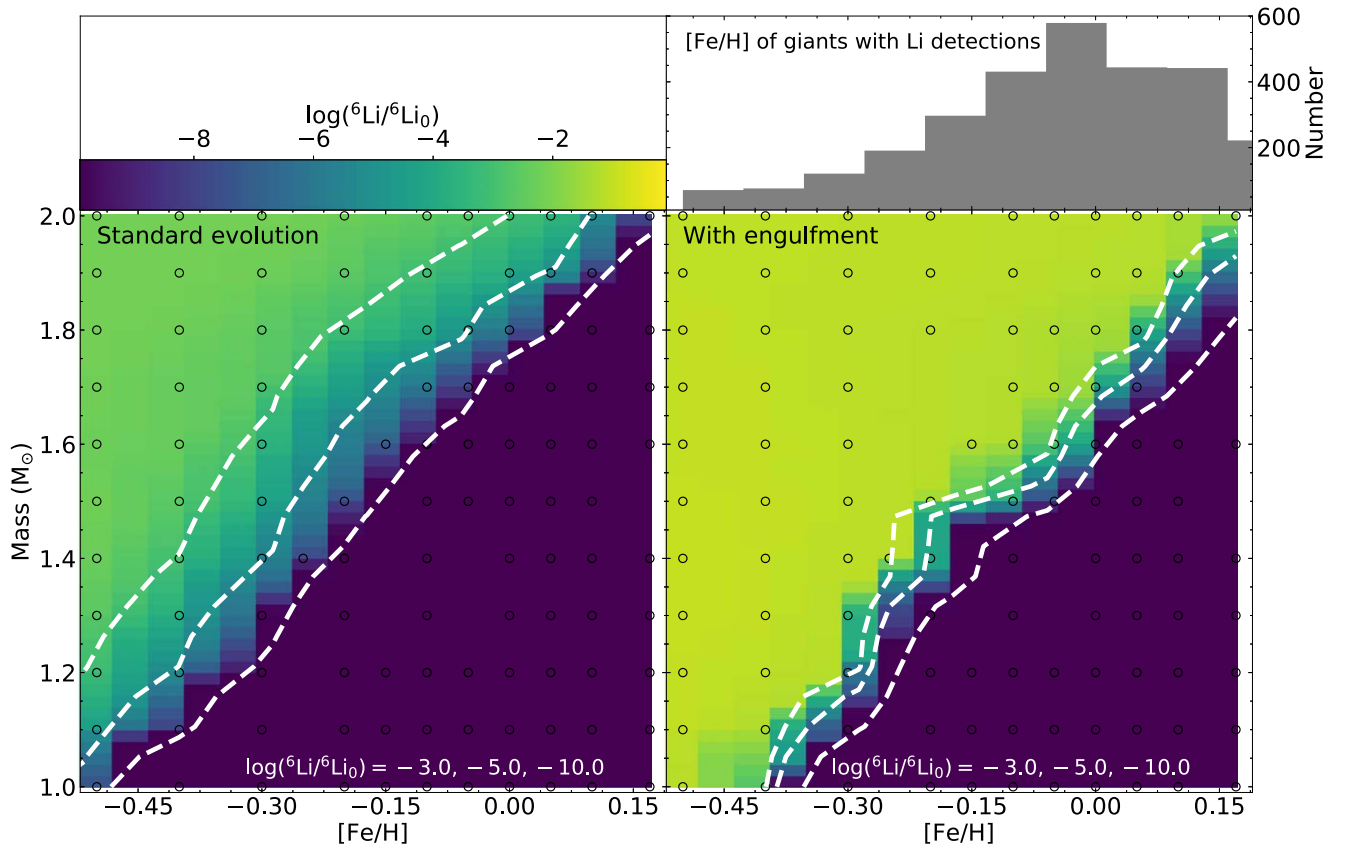
Figure 4. Top right panel: metallicity distribution of observed giants with measured ^{7}Li, which concentrate toward higher metallicities. Bottom left panel: standard surface ^{6}Li/^{6}Li$_0$ abundance of stars of different masses and metallicities. This map considers no engulfment of SSCs. Bottom right panel: surface ^{6}Li/^{6}Li$_0$ abundance of stars of different masses and metallicities after the engulfment of a 15 M_J brown dwarf enhanced in metal content. The three white contours indicate where $\log(^6$Li/^{6}Li$_0) = -3, -5$ and -10 from left to right. Stars of higher metallicities rapidly burn their ^{6}Li content and any additional ^{6}Li incorporated by the ingestion of SSCs.

the brown dwarf with high Z, while Earth-like planets barely increase the original ^{6}Li.

For these giants ^{6}Li burning can be significant during the dredge-up and RGB. We see this in the 1.7 $M_\odot$ star in Figure 3. Thus, there are some differences in the stellar ^{6}Li after engulfment when planets are accreted at different locations along the RGB. Later engulfment times imply larger ^{6}Li, a difference that can be considerable when burning is significant in the star. Notice, however, that even in the best-case scenario in terms of engulfment time, the values of ^{6}Li are still extremely low after burning proceeds.

The resulting ^{6}Li is mass and metallicity dependent. In Figure 3, we see almost no burning post-engulfment in the 1.8 $M_\odot$, [Fe/H] $= -0.5$ giant and severe burning in the 1.7 $M_\odot$, metal-rich star.

Figure 4 shows a map of ^{6}Li/^{6}Li$_0$, the ratio between current ^{6}Li abundance to the meteoritic ^{6}Li, in standard stars of different masses and metallicities, without planet engulfment. We obtain in our models the ^{6}Li abundance at the tip of the RGB in stars of the grid (small circles in the figure), that is then interpolated to produce the color-coded map. In metal-poor stars, a small amount of ^{6}Li is found in the surface, even without engulfment. However, metal-rich stars (solar metallicity and higher) reach the RGB with low ^{6}Li, which decreases even more after the first dredge-up where ^{6}Li is also burned under convective conditions, vanishing completely.

We present a similar map of ^{6}Li/^{6}Li$_0$ for stars of different masses and metallicities in Figure 4, bottom right panel, now

considering the engulfment of a 15 M_J brown dwarf enhanced in metals at the end of the first dredge-up.

Comparing this to the bottom left panel of Figure 4, ^{6}Li can increase significantly with engulfment. However, for metal-rich stars, the incorporated ^{6}Li is rapidly burned and would not be observed in the stellar surface. This becomes important when distinguishing ^{7}Li-enrichment mechanisms, since most of these giants are metal-rich.

We compiled a catalog of observed giants with measured ^{7}Li, where no upper limits are considered, and show their metallicities in the histogram of Figure 4, top right panel. These measurements are obtained from the literature, and as such are not homogeneous. Additionally, some of these sources only report their Li-rich giants.[6] As ^{7}Li-rich giants seem to be more metal-rich, this could bias our compilation to higher metallicities. The catalog includes giants from Gilroy (1989), Brown et al. (1989), Jasniewicz et al. (1999), Gonzalez et al. (2009), Kumar et al. (2011), Pace et al. (2012), Carlberg et al. (2012, 2016), Lebzelter et al. (2012), Martell & Shetrone (2013), Liu et al. (2014), Adamów et al. (2014), Böcek Topcu et al. (2015), Luck (2015), Delgado Mena et al. (2016), Casey et al. (2016), Smiljanic et al. (2018), and Deepak & Reddy (2019).

---

[6] In Aguilera-Gómez et al. (2016a) we find that not reporting the entire sample makes it harder to account for the full phenomenology creating Li-enriched giants.

In this histogram, most of the stars with measured ^{7}Li are metal-rich. The peak of this distribution is located at a metallicity at which ^{6}Li burns rapidly, with no ^{6}Li in the stellar surface, as we can see contrasting this distribution with the color map in the bottom panel. Thus, we would not expect to find ^{6}Li in most of the observed giants, even if they have engulfed an SSC previously. The limiting metallicity at which ^{6}Li could never be detected post-engulfment due to its rapid burning increases with mass.

If ^{6}Li is burned in the star the signal of SSCs would not be detected. In contrast, the ^{7}Li after engulfment could be preserved during the entire RGB phase if no extra mixing decreases its abundance. This could be the case for more metal-rich stars, where extra mixing seems to be less efficient (Shetrone et al. 2019) and suggests that even if the giant accreted a planet, its ^{7}Li abundance could be high, while its ^{6}Li remains low.

4. Discussion

As expected, ^{6}Li can increase in a low-mass giant after the engulfment of SSCs. However, ^{6}Li is rapidly burned in stars of higher metallicity, indicating that the absence of this isotope does not discard the possibility that the star accreted an SSC, but if there was an engulfment event, it did not occur recently. The destruction of this isotope at a faster rate than the ^{7}Li leads to low ^{6}Li, regardless of the $A(^7\text{Li})$, not rejecting the engulfment possibility (Drake et al. 2002). This point therefore becomes a crucial one in the quest for the sources of ^{7}Li enrichment in giants, as most of the giants that have measured ^{7}Li have higher metallicities. If ^{6}Li were to be seen at high metallicity, then its most likely explanation is a source other than an accreted SSC.

At the same time, only the ^{7}Li-rich giants with $A(^7\text{Li}) < 2.2$ can be explained by the engulfment of SSC (Aguilera-Gómez et al. 2016a). Therefore, the presence or absence of ^{6}Li in stars of higher ^{7}Li abundance (e.g., Monaco et al. 2014) does not give any information on this particular enrichment mechanism.

In contrast, if ^{6}Li is detected in a relatively metal-poor giant with $A(^7\text{Li}) < 2.2$, this could be due to the recent engulfment of an SSC. Engulfment could explain both the high ^{7}Li and ^{6}Li abundances at the same time, but there could also be independent explanations for the enrichment of each isotope.

From a purely observational point of view, detecting the ^{6}Li isotope can be particularly hard, as it manifests itself as a subtle asymmetry of the ^{7}Li line at $\sim$6708 Å. Even a Li isotopic ratio as high as solar can be hard to detect at solar-like metallicities due to convective line asymmetries and blends with other lines. There is a small region of parameter space where the increase in ^{6}Li could be detected, i.e., in higher-mass RGB stars engulfing brown dwarfs companions. These hypothetical detections of ^{6}Li would be especially interesting in giants with $A(^7\text{Li}) < 2.2$. Giants with more ^{7}Li (and stronger ^{7}Li lines, where the ^{6}Li could be more easily detected) can be excluded as engulfment candidates solely based on their ^{7}Li abundances (Aguilera-Gómez et al. 2016a).

Not only is the ^{6}Li detection observationally hard, but also, as the stellar mass increases, the lifetime a star spends on its RGB phase decreases considerably. Thus, it is very unlikely to find the higher-mass objects that could retain part of their ^{6}Li signature.

An interesting solar-metallicity Li-enriched giant is presented by Mott et al. (2017), who report a Li isotopic ratio close to the solar meteoritic ratio, and as such it is an interesting case to analyze. These high abundances are difficult to explain both with stellar flares and accretion of SSCs. To get to this very high ratio, a large amount of material would need to be accreted and, at solar metallicity, any ^{6}Li donated by a companion to the star is burned very rapidly. As such, we confirm the calculations by Mott et al. (2017) that led them to suggest that engulfment is an unlikely explanation for this particular star.

5. Summary

The fragile ^{6}Li isotope is destroyed at even smaller temperatures than ^{7}Li. As such, stellar evolution theory predicts giants with small ^{6}Li abundances. The ^{6}Li could increase after the engulfment of SSCs, making ^{6}Li to appear as a good diagnostic for an engulfment event in giants.

In this work, we modeled the ^{6}Li and $^6\text{Li}/^7\text{Li}$ of a giant, which increases after the engulfment of a companion. We demonstrate that metal-rich stars very rapidly burn this ^{6}Li. Given that no ^{6}Li can be found in metal-rich giants even after planet engulfment, its abundance should not be used as a way to distinguish between different ^{7}Li-enrichment mechanisms nor as a method to reject the planet engulfment hypothesis. Moreover, enrichment of ^{6}Li in low-mass metal-rich giants is likely not due to planet engulfment. There is only a very low probability that we find such an extremely recent engulfment event, where ^{6}Li is still not burned completely.

Stars with $A(^7\text{Li}) > 2.2$ could not be explained by planet accretion on the basis of their ^{7}Li alone. Thus, measurements of ^{6}Li in these stars do not indicate anything about the ^{7}Li-enrichment mechanism. In contrast, finding stars with high abundances of both ^{7}Li and ^{6}Li in a certain metallicity range could point to a recent engulfment event. However, a combination of mechanisms, one to enhance ^{7}Li and another to increase the ^{6}Li, is still possible, especially if the star is metal-rich and its ^{6}Li is much less likely to be explained by accretion.

In conclusion, we advise caution when using ^{6}Li as a diagnostic of engulfment or when using it to favor a scenario of ^{7}Li enrichment over others.

ORCID iDs

Claudia Aguilera-Gómez https://orcid.org/0000-0002-9052-382X
Julio Chanamé https://orcid.org/0000-0003-2481-4546
Marc H. Pinsonneault https://orcid.org/0000-0002-7549-7766

References

Adamów, M., Niedzielski, A., Villaver, E., Wolszczan, A., & Nowak, G. 2014, A&A, 569, A55

Aguilera-Gómez, C. 2018, External Mechanisms (Cham: Springer),

Aguilera-Gómez, C., Chanamé, J., Pinsonneault, M. H., & Carlberg, J. K. 2016a, ApJ, 829, 127

Aguilera-Gómez, C., Chanamé, J., Pinsonneault, M. H., & Carlberg, J. K. 2016b, ApJL, 833, L24

Böcek Topcu, G., Afşar, M., Schaeuble, M., & Sneden, C. 2015, MNRAS, 446, 3562

Brown, J. A., Sneden, C., Lambert, D. L., & Dutchover, E., Jr. 1989, ApJS, 71, 293

Brown, L., & Schramm, D. N. 1988, ApJL, 329, L103

Cameron, A. G. W., & Fowler, W. A. 1971, ApJ, 164, 111

Carlberg, J. K., Cunha, K., Smith, V. V., & Majewski, S. R. 2012, ApJ, 757, 109

Carlberg, J. K., Smith, V. V., Cunha, K., & Carpenter, K. G. 2016, ApJ, 818, 25

Casey, A. R., Ho, A. Y. Q., Ness, M., et al. 2019, ApJ, 880, 125

Casey, A. R., Ruchti, G., Masseron, T., et al. 2016, MNRAS, 461, 3336

Charbonnel, C., Balachandran, S. C., et al. 2000, A&A, 359, 563

Chaussidon, M., & Robert, F. 1998, E&PSL, 164, 577

Chaussidon, M., & Robert, F. 1999, Natur, 402, 270

Coc, A., Uzan, J.-P., & Vangioni, E. 2014, JCAP, 10, 050

Deepak, & Reddy, B. E. 2019, MNRAS, 484, 2000

Delgado Mena, E., Tsantaki, M., Sousa, S. G., et al. 2016, A&A, 587, A66

Drake, N. A., de la Reza, R., da Silva, L., & Lambert, D. L. 2002, AJ, 123, 2703

Fields, B. D., & Olive, K. A. 1999, NewA, 4, 255

Gilroy, K. K. 1989, ApJ, 347, 835

Gonzalez, O. A., Zoccali, M., Monaco, L., et al. 2009, A&A, 508, 289

Jasniewicz, G., Parthasarathy, M., de Laverny, P., & Thévenin, F. 1999, A&A, 342, 831

Kumar, Y. B., Reddy, B. E., & Lambert, D. L. 2011, ApJL, 730, L12

Lamia, L., Spitaleri, C., Pizzone, R. G., et al. 2013, ApJ, 768, 65

Lebzelter, T., Uttenthaler, S., Busso, M., Schultheis, M., & Aringer, B. 2012, A&A, 538, A36

Liu, Y. J., Tan, K. F., Wang, L., et al. 2014, ApJ, 785, 94

Luck, R. E. 2015, AJ, 150, 88

Martell, S., Simpson, J., Balasubramaniam, A., et al. 2020, arXiv:2006.02106

Martell, S. L., & Shetrone, M. D. 2013, MNRAS, 430, 611

Martin, E. L., Rebolo, R., Casares, J., & Charles, P. A. 1994, ApJ, 435, 791

Meneguzzi, M., Audouze, J., & Reeves, H. 1971, A&A, 15, 337

Monaco, L., Boffin, H. M. J., Bonifacio, P., et al. 2014, A&A, 564, L6

Montes, D., & Ramsey, L. W. 1998, A&A, 340, L5

Mott, A., Steffen, M., Caffau, E., Spada, F., & Strassmeier, K. G. 2017, A&A, 604, A44

Pace, G., Castro, M., Meléndez, J., Théado, S., & do Nascimento, J.-D., Jr. 2012, A&A, 541, A150

Pinsonneault, M. 1997, ARA&A, 35, 557

Pinsonneault, M. H., Kawaler, S. D., Sofia, S., & Demarque, P. 1989, ApJ, 338, 424

Prantzos, N. 2012, A&A, 542, A67

Prantzos, N., de Laverny, P., Guiglion, G., Recio-Blanco, A., & Worley, C. C. 2017, A&A, 606, A132

Proffitt, C. R., & Michaud, G. 1989, ApJ, 346, 976

Sackmann, I.-J., & Boothroyd, A. I. 1992, ApJL, 392, L71

Shetrone, M., Tayar, J., Johnson, J. A., et al. 2019, ApJ, 872, 137

Siess, L., & Livio, M. 1999, MNRAS, 308, 1133

Smiljanic, R., Franciosini, E., Bragaglia, A., et al. 2018, A&A, 617, A4

Takeda, Y., & Tajitsu, A. 2017, PASJ, 69, 74

Tayar, J., Ceillier, T., García-Hernández, D. A., et al. 2015, ApJ, 807, 82

Yan, H.-L., Shi, J.-R., Zhou, Y.-T., et al. 2018, NatAs, 2, 790